ELSEVIER

Journal of Chromatography A, 702 (1995) 113–123

JOURNAL OF CHROMATOGRAPHY A

Model for ion-exchange equilibria of macromolecules in preparative chromatography

Yonglong Li, Neville G. Pinto*

Department of Chemical Engineering, University of Cincinnati, Cincinnati, OH 45221-0171, USA

Abstract

An adsorption model based on the stoichiometric displacement principle was developed for the non-linear ion-exchange of macromolecules. In this model, the adsorbed phase is a non-ideal surface solution in equilibrium with a non-ideal bulk liquid, and non-idealities in both phases are quantified in terms of activity coefficient corrections. The equilibrium model accounts for the shape and charge of the adsorbates, lateral interactions on the surface and the effects of modulating salts. Practical methods were developed for evaluating model coefficients, and the model was applied to overloaded elution chromatography of bovine serum albumin. It is shown that non-idealities in the liquid phase and lateral interactions on the surface strongly influence elution profiles.

1. Introduction

HPLC has been widely employed for protein separations on both the analytical and preparative scales [1]. Overload elution and displacement modes of operation are often used to increase productivity in preparative processes [2–6]. In contrast to analytical operations, in which the linear equilibrium description is adequate, the non-linear isotherm region is invariably important for overloaded chromatography, owing to the larger column loads. The lack of an appropriate model to describe adequately non-linear equilibria has significantly impeded the design and optimization of preparative processes.

The Langmuir isotherm is a frequently invoked equilibrium model, despite its inadequacy and thermodynamic inconsistency [7,8]. In ion-exchange chromatography of proteins, a modulator, often a salt, is frequently added to the mobile phase in fairly high concentrations (up to 1 M) to modulate the protein retention [9]. As a result, induced salt gradient phenomena are observed [10,11]. Protein molecules have complex three-dimensional structures, relatively high molecular masses and pH-dependent surface charge characteristics. Enthalpy changes accompanying the adsorption process can be endothermic or exothermic, and may be dependent on the coverage [12,13]. In the light of the complexity of the protein ion-exchange process, the traditional Langmuir model cannot adequately describe the equilibrium behavior. Many researchers have been striving to propose more appropriate theoretical frameworks to incorporate factors such as the presence of modulators, lateral interactions, effective charge and size exclusion [14–18]. These efforts have been summarized in a previous paper [19].

In this paper, we present recent developments in our continuing efforts to develop the non-ideal

* Corresponding author.

0021-9673/95/$09.50 © 1995 Elsevier Science B.V. All rights reserved
SSDI 0021-9673(94)01281-4

surface solution (NISS) model for protein ion exchange. Borrowing on concepts developed in solution thermodynamics and the adsorption of gases on solids, this model attempts to incorporate, in a thermodynamically rigorous manner, the major features of protein ion exchange. The emphasis of the current contribution is non-idealities in the mobile phase, the importance of lateral interactions and the evaluation of model parameters. Both equilibrium and column behavior of BSA have been investigated.

2. Theory

2.1. Brief description of the NISS model

In a previous paper [19] we provided a detailed description of the NISS model. In the following description, we summarize the main features and describe the modifications incorporated.

In the NISS model, the adsorption $n-1$ macromolecules, $N_1, N_2, \ldots, N_{n-1}$, is considered in the presence of a small counterion (salt) N_n, called the modulator. As per the stoichiometric displacement model (SDM) [16], the mechanism of adsorption is stoichiometric ion exchange with complete co-ion exclusion. The equilibrium distribution for the system is described by

$$\begin{aligned} z_1 N_n^s + N_1 &\rightleftharpoons z_1 N_n + N_1^s \\ z_2 N_n^s + N_2 &\rightleftharpoons z_2 N_n + N_2^s \\ &\vdots \\ z_{n-1} N_n^s + N_{n-1} &\rightleftharpoons z_{n-1} N_n + N_{n-1}^s \end{aligned}$$

For each of these ion-exchange "reactions", the equilibrium constants are related to the species activities by

$$K_i = \frac{(a_n)^{z_i} a_i^s}{(a_n^s)^{z_i} a_i} \quad i = 1, 2, \ldots, n-1 \tag{1}$$

In the adsorbed phase,

$$a_i^s = \gamma_i^s n_i^s \quad i = 1, 2, \ldots, n \tag{2}$$

In the mobile phase,

$$a_i = \gamma_i c_i \quad i = 1, 2, \ldots, n \tag{3}$$

The activity coefficient of the protein in the mobile phase is assumed to be unity since, in most cases, protein solutions are dilute. For what is usually considered a fairly "high" mobile phase protein concentration, say 100 mg/ml, the molar concentration is still low, owing to the high molecular mass of the protein. In contrast, the modulator molar concentration can be orders of magnitude higher. As a result, liquid-phase non-idealities originating from the modulator cannot in general be neglected. With these considerations, Eq. 1 becomes

$$K_i = \frac{(c_n \gamma_n)^{z_i} \gamma_i^s n_i^s}{(\gamma_n^s n_n^s)^{z_i} c_i} \quad i = 1, 2, \ldots, n-1 \tag{4}$$

By definition,

$$\sum_i^n n_i^s = n^s \tag{5}$$

where n^s is the total ion-exchange capacity of the adsorbent. Eqs. 4 and 5, in conjunction with appropriate equations for the activity coefficients in the surface phase and for the modulator in the liquid phase, constitute the equilibrium model.

2.2. Modulator activity coefficients

A variety of methods are available to estimate activity coefficients in electrolyte solutions [20–25]. Among these, the method developed by Bromley [21] has been found to be effective for strong electrolytes up to an ionic strength of about 6. In terms of the ionic strength of the liquid, the Bromley equation is expressed as

$$\log \gamma_{\pm} = \frac{-0.511 I^{1/2}}{1 + I^{1/2}} + \frac{(0.06 + 0.6B)|z_+ z_-| I}{\left(1 + \frac{1.5}{|z_+ z_-|} I\right)^2} + BI \tag{6}$$

This equation contains a single coefficient B, which is readily available for all salts commonly used as modulators in protein ion-exchange chromatography.

2.3. Surface activity coefficients

As before [19], Talu and Zwiebel's [26] equation is employed for the calculation of the activity coefficients in the surface phase:

$$\ln \gamma_i^s = -s_i \ln\left(\sum_{j=1}^{n} \omega_j \alpha_{ij}\right) + s_i - s_i \sum_{j=1}^{n} \frac{\omega_j \alpha_{ij}}{\sum_{k=1}^{n} \omega_k \alpha_{kj}} \qquad i = 1, 2, \ldots, n \quad (7)$$

where s_i is the adsorbate shape factor and ω_j is the surface fraction, defined as

$$\omega_j = \frac{s_j x_j^s}{\sum_{k=1}^{n} s_k x_k^s} \quad (8)$$

α_{ij} is the Boltzmann weighting factor for local compositions. It is calculated using Wilson's method [27] for incorporating differences in intermolecular forces between components of the adsorbed phase; α_{ij} is related to the average lateral interaction energy between segments of nearest-neighbor molecules (e_{ii} or e_{jj}) by

$$\alpha_{ij} = \exp\left[-\frac{\sigma}{2}(e_{ij} - e_{jj})/kT\right] \quad (9)$$

where σ is the coordination number for the adsorbed segments. The energy of interaction parameters e_{jj} and e_{ij} are functions of the spreading pressure. Talu and Zwiebel [26] showed that at low temperatures e_{jj} can be calculated from pure component isosteric heat of adsorption data:

$$e_{jj} = \frac{q_{j\pi}^{st} - q_{j0}^{st}}{\frac{\sigma}{2} \cdot MS_j} \quad (10)$$

where $q_{j\pi}^{st}$ is the isosteric heat of adsorption of pure j at the same spreading pressure as the mixture and q_{j0}^{st} is the isosteric heat of adsorption at zero spreading pressure. The cross-energy parameters are calculated from

$$e_{ij} = (e_{ii}e_{jj})^{1/2}(1 - \beta_{ij}) \quad (11)$$

where β_{ij} is an empirical factor that accounts for differences in size and adsorptive properties of the molecules.

2.4. Model for chromatographic column

The NISS equilibrium model was combined with a kinetic model for a column packed with a porous adsorbent to provide a mathematical description of the chromatographic process. The kinetic description was adapted from Phillips et al. [28], and neglects the effects of axial dispersion. For a species i, the column equations are

$$\frac{\partial c_i}{\partial \tau} + \frac{\partial c_i}{\partial X} + \phi \cdot \frac{\partial \bar{n}_i}{\partial \tau} = 0 \qquad i = 1, 2, \ldots, n \quad (12)$$

$$\frac{\partial \bar{n}_i}{\partial \tau} = St_i(n_i^s - \bar{n}_i) \qquad i = 1, 2, \ldots, n \quad (13)$$

where

$$\tau = \frac{u_0 t}{L}; \quad X = \frac{1}{L}; \quad St_i = \frac{f_i L}{u_0}$$

For a spherical adsorbent, with the liquid-phase mass-transfer resistance assumed to be negligible and using Glueckauf's [29] linear driving force approximation, f_i is related to the protein diffusivity in the particle, $\bar{D}_i$, by

$$f_i = \frac{15\bar{D}_i}{R_p^2} \quad (14)$$

For the isocratic elution mode, the initial and boundary conditions are

$$c_i = \bar{n}_i = 0 \qquad \text{at } \tau = 0, 0 \le X \le 1 \quad i = 1, 2, \ldots, n-1 \quad (15)$$

$$c_n = c_{nF} \text{ and } \bar{n}_n = n^s \quad \text{at } \tau = 0, 0 \le X \le 1 \quad (16)$$

$$c_i = c_{iF} \qquad \text{at } X = 0, 0 \le \tau \le \tau_{feed} \quad i = 1, 2, \ldots, n \quad (17)$$

$$c_i = 0 \qquad \text{at } X = 0, \tau \ge \tau_{feed} \quad i = 1, 2, \ldots, n-1 \quad (18)$$

$$c_n = c_{nF} \qquad \text{at } X = 0, \tau \ge \tau_{feed} \quad (19)$$

$$\left.\frac{\partial c_i}{\partial X}\right|_{X=1} = 0 \qquad \text{at } X = 1, \tau \ge \tau_{feed} \quad i = 1, 2, \ldots, n \quad (20)$$

The coupled partial differential equations were solved numerically using a finite difference scheme. The set of non-linear isotherm equations were solved with a commercial non-linear equation solver package using the Powell hybrid method [30].

3. Experimental

3.1. Materials and apparatus

BSA was obtained from Sigma (St. Louis, MO, USA). Matrex PAE-1000 (a weak anion exchanger, 10 μm diameter, 1000 Å average pore size) was purchased from Amicon (Danvers, MA, USA), and was slurry packed into 0.46 cm I.D. columns at a maximum pressure of 4000 p.s.i. with a Haskel air-driven pump (Alltech, Deerfield, IL, USA). Sodium chloride, silver nitrate, sodium azide and imidazole were obtained from Aldrich (Milwaukee, WI, USA) and hydrochloric acid and methanol from Fisher Scientific (Fair Lawn, NJ, USA). All reagents were used as received.

The chromatographic system for the frontal and elution experiments included an SP8800 gradient HPLC pump (Spectra-Physics, San Jose, CA, USA), a Model 2550 UV–Vis detector (Varian, Sunnyvale, CA, USA) and an HP 3396A integrator (Hewlett-Packard, Palo Alto, CA, USA). The protein concentration was measured with a UV-160/CL-750 spectrophotometer (Shimadzu, Kyoto, Japan).

3.2. Effective protein charge and equilibrium constant

The effective charge (z_i) and equilibrium constant (K_i) of BSA were as measured by linear isocratic elution on a 25 cm × 0.46 cm I.D. column. Details for these experiments have been reported earlier [19]. The salt (NaCl) range used was 0.15–0.4 M and experiments were performed at a number of temperatures in the range 6.1–35.5°C.

3.3. Isotherm measurements and equilibrium constant

BSA adsorption isotherms were measured at different sodium chloride concentrations at room temperature by the batch method. PAE-1000 was first weighed into test-tubes, then a known volume of protein solution at known salt and protein concentrations and pH 7 was added to the test-tubes with a syringe. The test-tubes were sealed with Parafilm and placed in a shaker for 24 h. Preliminary experiments had established that equilibrium can be reached in 8–10 h. Special attention was paid to the low protein concentration region because the equilibrium constant K_i was calculated from the data in this region. After equilibration, the slurry solution was centrifuged at 5000 rpm, and the clear solution was analyzed with a UV spectrophotometer at 280 or 310 nm. The equilibrium distribution was calculated from a mass balance.

3.4. Resin capacity

The capacity of the anion exchanger was measured by a procedure similar to that employed by Bentrop and Engelhardt [31], in which the column was first equilibrated with buffer solutions containing Cl^- at pH 7. Subsequent to rinsing the column with deionized water, sodium nitrate solution of known concentration was introduced; a low flow-rate, selected after preliminary experiments, was used to minimize mass-transfer effects. The column effluent was collected, and silver nitrate was used to titrate the Cl^- ions. The total capacity was then back-calculated from an equivalency balance.

3.5. Stanton number

The Stanton number for the column was determined from isocratic elution experiments with BSA on a 25 cm × 0.46 cm I.D. column. The experiments were performed at room temperature using a salt concentration of 0.35 M. A 20-μl volume of 5 mg/ml BSA solution was injected into the column and the response was

monitored at 280 nm. A flow-rate range of 0.5–2.5 ml/min was used.

4. Results and discussion

4.1. NISS parameter estimation

For each protein species being considered, the NISS model requires that three coefficients be evaluated: K_i, z_i and S_i. In addition, the isosteric heat of adsorption must be known as a function of surface coverage, and the total capacity of the support n^s must also be available. Previously [19], we described methods for evaluating these coefficients and reported experimental values for BSA on PAE-1000, with NaCl as the modulator. Here we investigated how removing the assumption of solution ideality will affect parameter estimation.

The equilibrium constant K_i and the effective charge z_i can be evaluated from linear isocratic elution data. From Eq. 4, it can be shown that for this mode of chromatography

$$\ln k_i' = \ln[\phi(n^s)^{z_i} K_i] - z_i \ln(c_n \gamma_n) \quad (23)$$

Fig. 1 shows a typical plot of Eq. 23 for BSA. Two lines are shown, both obtained from the same experimental data. In one case the liquid solution was assumed to be ideal, whereas for the other the Bromley equation (Eq. 6) was used to correct for liquid non-ideality. Since the slope of these lines gives z_i and the intercept gives K_i, it appears that whereas z_i is essentially unaffected by liquid non-ideality, K_i is severely influenced. Fig. 2 shows the value of z_i obtained in experiments at other temperatures, with and without the activity coefficient correction. In all cases a z_i value of 4.8 was obtained. These data confirm that z_i is independent of the liquid activity coefficient correction. It is also interesting that, within the temperature range studied, z_i is essentially independent of temperature, indicating that temperature has a secondary influence when compared with pH and modulator [32].

Fig. 3 shows the values of K_i obtained from the elution experiments, with and without the correction for liquid-phase non-ideality. Also plotted are values obtained from independent batch experiments at various modulator concentrations. The match between the two sets indicates that the elution method is reliable for obtaining K_i. It should be noted that the modulator concentration axis (abscissa) only applies to the batch data; for the elution data the points have been separated for clarity only.

The results in Fig. 3 clearly demonstrate that liquid-phase non-ideality can have a strong effect on K_i. Neglecting its influence would, in this

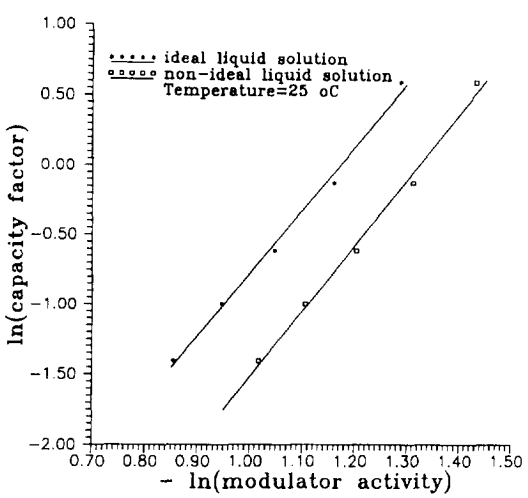

Fig. 1. Effective charge of BSA for ideal liquid solution and non-ideal liquid solution.

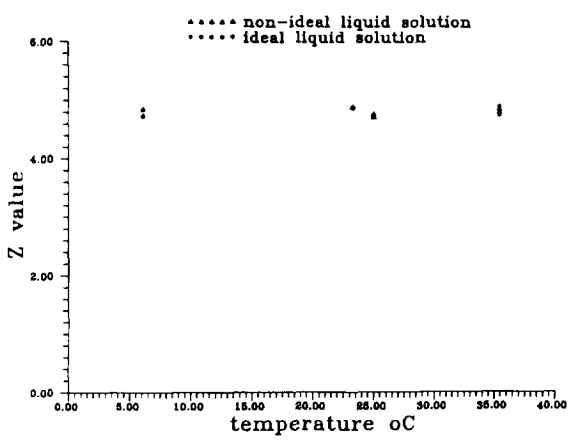

Fig. 2. Effective charge of BSA at different temperatures.

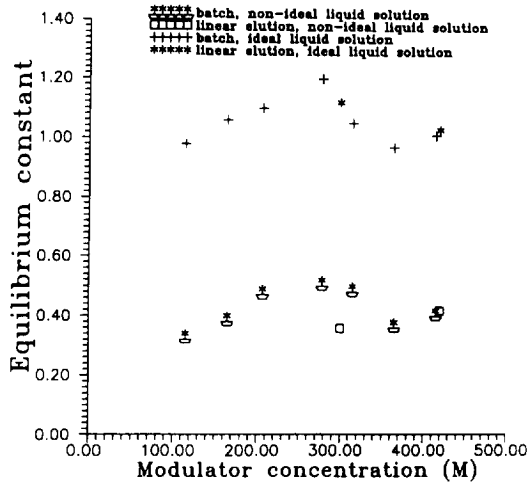

Fig. 3. Equilibrium constant of BSA at different modulator concentrations.

case, lead to an over-estimate of K_i of well over 200%.

The influence of liquid-phase non-ideality can be expected to be even stronger if modulator ions of higher valency are used. Fig. 4 shows the influence of modulator charge on liquid activity coefficient; values in this figure were calculated keeping B (Eq. 6) constant at the value for NaCl and changing the z_i for the counter ion. It should be noted that the further the value of the activity

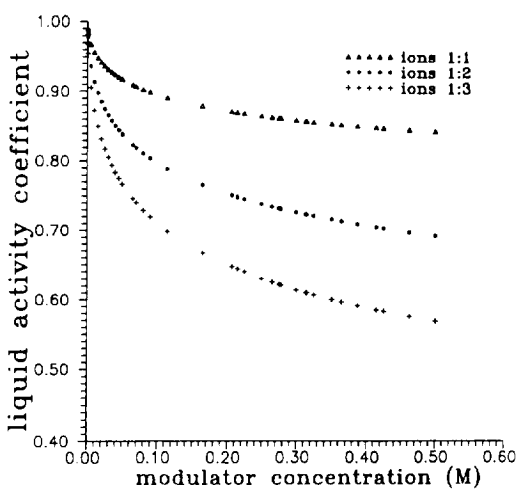

Fig. 4. Effect of type of counter ions on liquid activity coefficient.

coefficient is from 1, the stronger the influence of the liquid phase on K_i.

Fig. 4 also provides an explanation for the observed independence of z_i from the liquid activity coefficient. The modulator concentrations used for the evaluation of z_i (Fig. 1) were always higher than 0.2 M. In this range, the liquid activity coefficient is essentially constant for NaCl (Fig. 4, 1:1). Hence, this coefficient shifts the points in Fig. 1 from their ideal solution value by approximately the same amount at every modulator concentration in the experimental range. It should be noted, however, that at lower concentrations the liquid activity coefficient is a strong function of the concentration. Hence it is to be expected that z_i will not be constant at lower concentrations, which is consistent with experimental observations reported in the literature [32].

The shape factor in Eq. 7 is defined as

$$S_p = \frac{L_p}{L_s} \tag{24}$$

where L_p is the outer free perimeter of the protein and L_s the outer free perimeter of a standard molecule [33]. Selecting the modulator ion as the standard ion, and assuming all adsorbates to have a square imprint,

$$L_s = 4\left(\frac{A_s}{n^s}\right)^{1/2} \tag{25}$$

$$L_p = 4\left(\frac{A_s}{n^p}\right)^{1/2} \tag{26}$$

where A_s is the specific area of the adsorbent and n^s and n^p are the saturation capacities of the adsorbent for the modulator and protein, respectively. The capacity for the modulator is the same as the ion-exchange capacity of the adsorbent, because all the ion-exchange sites are accessible to the small modulator ions [31]. For the proteins, in contrast, only a small fraction of the total ion-exchange sites are accessible. For example, for BSA on PAE-1000, at pH 7 and room temperature, the saturation capacity was found to be 150 mg/g. Using the effective charge of 4.8, this translates into a utilized capacity of approximately 3% of the total capacity.

Substituting Eqs. 25 and 26 into Eq. 24, and using the experimentally obtained ion-exchange capacity of the adsorbent of 360 μequiv./g and the protein saturation capacity at pH 7, a shape factor of 5.5 was calculated. This value is remarkably close to the best-fit value of 5.6 obtained by us earlier [19] from room-temperature isotherm data.

Previously [19], we had measured the dependence of the isosteric heat of adsorption of BSA on PAE-1000 at a very low modulator concentration. This was done by obtaining the adsorption isotherms at a number of temperatures and then calculating the isosteric heat through a Clausius–Clapeyron type equation. With this approach, it was shown that the isosteric heat of adsorption is a linear function of the surface mole fraction of BSA. Although this approach works well, it is experimentally tedious.

For this work, we chose an alternative approach. Based on our earlier results [19], we assume the linear dependence of isosteric heat on protein coverage holds at other modulator concentrations, i.e.,

$$q_{i\pi}^{st} - q_{i0}^{st} = mx_i^s \tag{27}$$

where the coefficient m will change with modulator concentration. This coefficient can be obtained at a given modulator concentration from the best fit of the NISS model to an experimentally measured adsorption isotherm at this concentration. Fig. 5 are the experimental isotherms, the best-fit simulations and the corresponding m values for modulator concentrations of 0.21 and 0.39 M. The advantage of this method is that isotherms have to be measured only at one temperature, instead of a series of temperatures, as was done earlier [19].

4.2. Column behavior

Experimental isocratic elution peaks of BSA were compared with predictions of column simu-

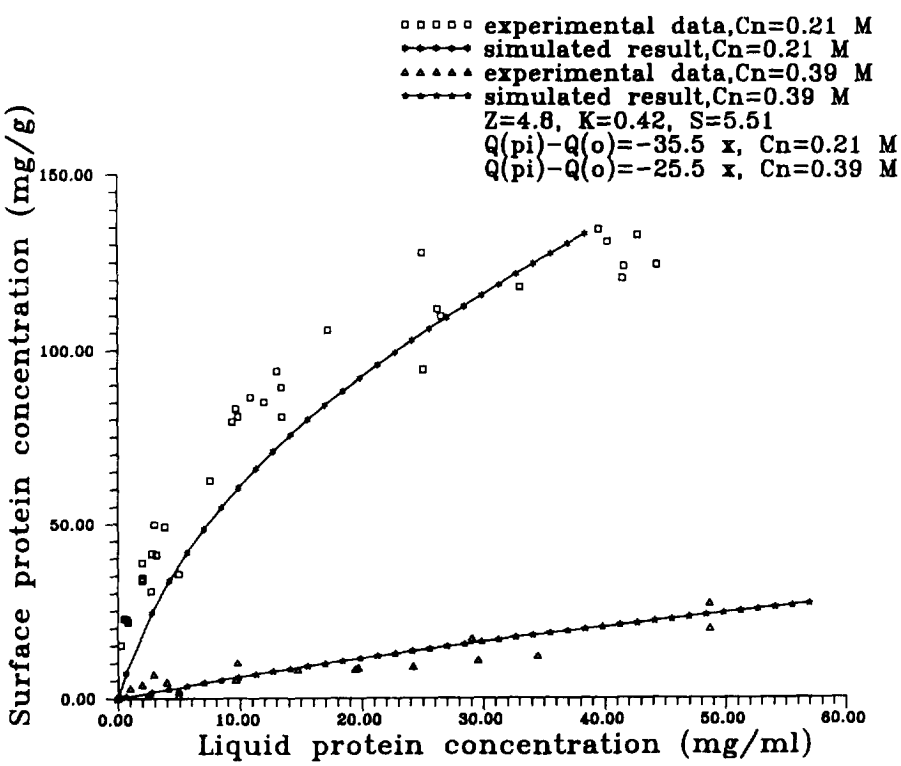

Fig. 5. BSA equilibrium isotherms at 0.21 and 0.39 M NaCl concentrations.

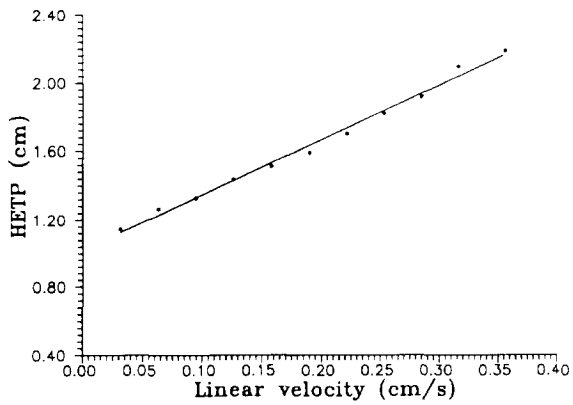

Fig. 6. Relationship between HETP and fluid linear velocity.

lations to establish the validity of the NISS equilibrium description. The mass transfer resistance in the particle phase (Stanton number) was estimated from the elution experiments described earlier, using the moment method of Ma and Lin [34]. According to this method, a plot of HETP vs. fluid velocity should give a straight line. Fig. 6 shows the plot for BSA. From the slope of this line, the BSA diffusivity in the particle was calculated and substituted in Eq. 14 to obtain a Stanton number of 20.

Using the measured equilibrium and kinetic parameters (Table 1), isocratic elution peaks of BSA were simulated at two salt concentrations, 0.21 and 0.39 *M*. Figs. 7–9 are comparisons of these predictions with experimental results. Fig. 7 is the comparison for a column loading of 100 μl of 61.37 mg/ml BSA at 0.39 *M* NaCl. In general, the model predicts the experimental response reasonably well. The peak retention

Table 1
Model parameters for column simulations

Parameter	Value
K_i	0.42
z_i	4.8
S_i	5.51
n^*	360 μequiv./g
St_i	20
$q_{\pi}^{st} - q_0^{st}$	$-25.5x$ at 0.39 *M* NaCl
	$-35.5x$ at 0.21 *M* NaCl

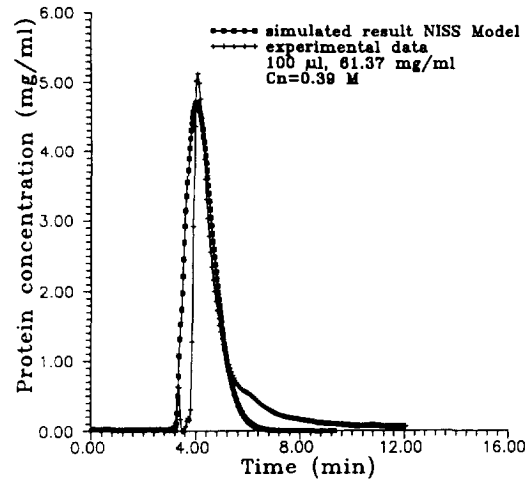

Fig. 7. Comparison of experimental and NISS simulation peaks (100 μl, $C_n = 0.39$ *M*).

times of the two peaks correspond, and peak shapes are characterized by a sharpening front and tailing rear. Also, at a higher column loading (Fig. 8) and lower salt concentration (Fig. 9) the correspondence between the simulated and experimental peaks is maintained.

The differences observed between experimental and simulated peaks are primarily attributed to poor estimation of the kinetic effects and the presence of an impurity or variant of BSA. In

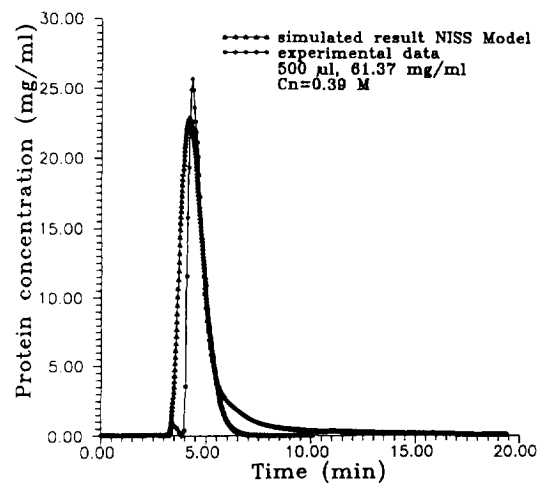

Fig. 8. Comparison of experimental and NISS simulation peaks (500 μl, $C_n = 0.39$ *M*).

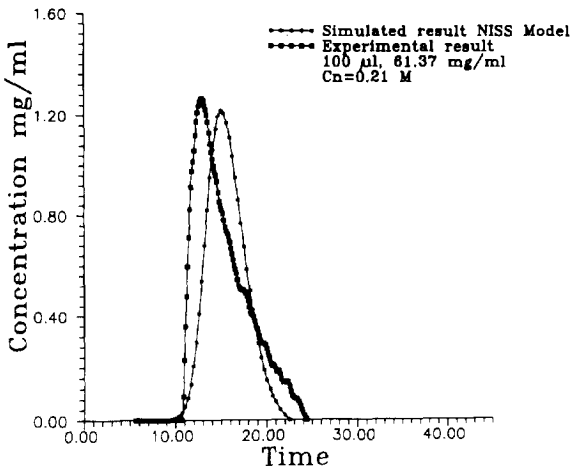

Fig. 9. Comparison of experimental and NISS simulation peaks (100 μl, $C_n = 0.21$ M).

Figs. 7–9 the experimental peaks are all higher than the simulated peaks, and their fronts are sharper. This can be accounted for by small changes in the Stanton number. For example, Fig. 10 illustrates the sensitivity of the peak shape to the Stanton number; a relatively small change from 15 to 20 results in a significant sharpening of the peak and, consequently, a greater peak height. To match the experimental and simulated peak heights in Figs. 7–9 would require only a small change in the Stanton number, one that is within the limit of precision of the estimation method (Fig. 6). Therefore, we believe that this discrepancy is not rooted in problems with the NISS model, but stems from an underestimate of the Stanton number by the moment method [34].

An underestimate of the Stanton number should, however, also result in a simulated peak that has a more diffuse rear than is obtained experimentally . From Figs. 7–9, it is clear that the opposite is observed. This is explained by the presence of an impurity or variant of BSA in the mixture. Fig. 11 shows an isocratic chromatogram of BSA at 0.29 M NaCl. At this modulator concentration, the peak for the impurity (or variant) is clearly indicated. In Figs. 7–9, the region of greatest discrepancy between the rears of the simulated and experimental peaks is at the lower concentrations where the impurity appears.

The importance of accounting for lateral interactions and solution non-ideality for BSA is best illustrated by showing predictions in the absence of these factors. Fig. 12 shows a comparison of the experimental and predicted peaks when lateral interactions are not considered (ideal surface phase). Neglect of the surface repulsive forces between adsorbed BSA molecules results

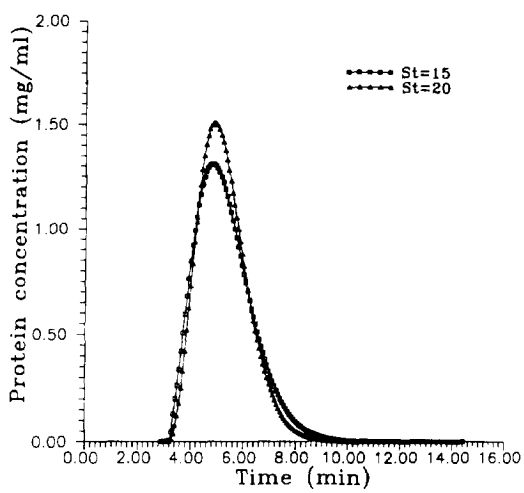

Fig. 10. Effect of Stanton number on column profiles.

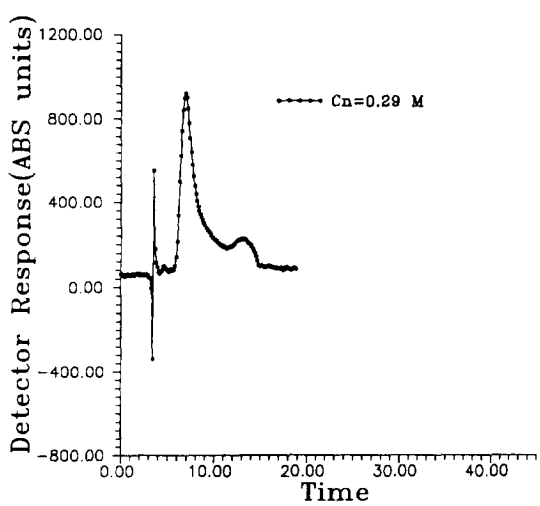

Fig. 11. Isocratic elution of BSA at 0.3 M NaCl.

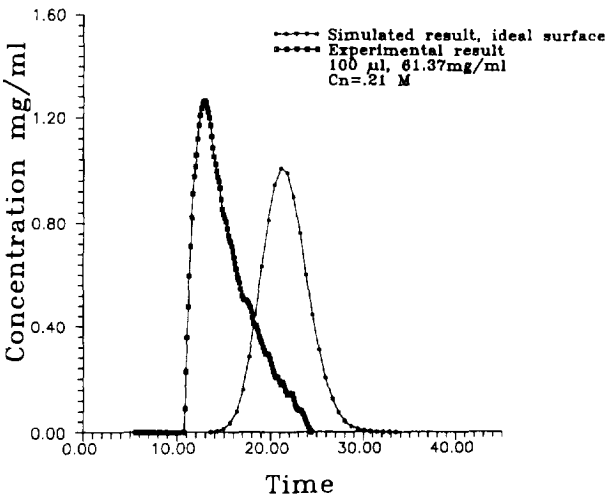

Fig. 12. Predicted BSA elution peak with lateral interactions neglected.

in the prediction of a higher than actual adsorption capacity and, therefore, a significantly longer than observed retention time. Equally poor predictions are obtained if the liquid phase is assumed to be ideal. In this case, as was discussed earlier (Fig. 3), the equilibrium constant is over-estimated. Consequently as illustrated in Fig. 13, peak retention times much higher than observed are obtained.

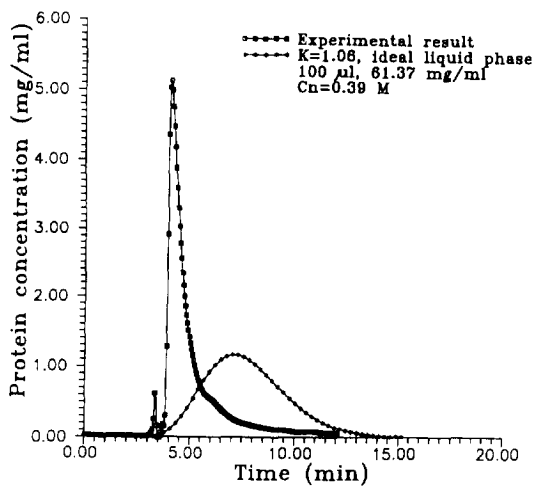

Fig. 13. Predicted BSA elution peak assuming ideal liquid solution.

5. Conclusions

The NISS model provides an effective and thermodynamically consistent approach to modeling protein adsorption for overloaded ion-exchange chromatography. The equilibrium coefficients of this model are conveniently calculated through a combination of elution and batch isotherm experiments. Using BSA as the probe molecule, it has been shown that the prediction of column behavior requires the incorporation of liquid-phase non-idealities; the relatively high modulator concentrations typically encountered in ion-exchange chromatography result in highly non-ideal liquid phases that influence binding strength. Also, lateral interactions on the surface cannot be ignored, and these are a function of surface coverage and modulator concentration.

Symbols

A	specific area of the resin
a_i	activity
B	Bromley constant
c_i	mobile phase concentration
$c_{i\mathrm{F}}$	mobile phase concentration in the feed
D_i	effective diffusion coefficient
e_{ij}	lateral interaction potential between segment of molecules i and j
f	effective mass transfer coefficient
I	ionic strength
k	Boltzmann constant
k_i'	column capacity factor for species i
K_i	equilibrium constant
l	column length
L	characteristic column length
L_p	protein outer free perimeter
L_s	salt outer free perimeter
m	slope coefficient in Eq. 27
M	Avogadro's number
n	number of species
$\bar{n}_i$	average concentration of species i on surface
n^s	total ion-exchange capacity
n^p	maximum protein capacity
n_i^s	concentration of species i on surface
N_i	adsorbate i

$q_{j\pi}^{st}$ isosteric heat at spreading pressure π
q_{j0}^{st} isosteric heat at spreading pressure zero
R_p radius of particle
S_i shape factor
Sk_i Stanton number for component i
t time
T absolute temperature
u_0 linear velocity
x coverage in mole fraction
X dimensionless length
z_i effective charge

Greek symbols

α_{ij} Boltzmann weighting factors for local segment compositions
β_{ij} empirical factor
ϕ column phase ratio
ω_j surface fraction
γ activity coefficient
σ coordination number
τ dimensionless time

Subscripts

i index for component i
j index for component j
k index for component k
F feed
n modulator
p protein
s salt or specific

Superscripts

s surface phase
st isosteric

Acknowledgement

This work was supported in part by Grant No. CTS-9207631 from the National Science Foundation. This support is gratefully acknowledged.

References

[1] F.E. Regnier, *Chromatographia*, 24 (1987) 241.
[2] Cs. Horváth, J. Frenz and Z. El Rassi, *J. Chromatogr.*, 255 (1983) 273.
[3] A.M. Katti, and G. Guiochon, *J. Chromatogr.*, 499 (1990) 21.
[4] J.H. Knox and H.M. Pyper, *J. Chromatogr.*, 363 (1986) 1.
[5] A. Jungbauer, *J. Chromatogr.* 639 (1993) 3.
[6] G. Subramanian and S.M. Cramer, *Biotechnol. Prog.*, 5 (1989) 92.
[7] P.K. de Bokx, P.C. Baarslag and H.P. Urbach, *J. Chromatogr.*, 594 (1992) 9.
[8] D.M. Ruthven, *Principles of Adsorption and Adsorption Processes*, Wiley, New York, 1984.
[9] A. Velayudhan and M.R. Ladisch, *Anal. Chem.*, 63 (1991) 2028.
[10] E.A. Peterson, *Anal. Chem.*, 90 (1978) 767.
[11] J.A. Gerstner and S.M. Cramer, *Biotechnol. Prog.*, 8 (1992) 540.
[12] W. Norde, *J. Dispers. Sci. Technol.*, 13 (1992) 363.
[13] P.G. Koutsoukos, W. Norde and J. Lyklema, *J. Colloid Interface Sic.*, 95 (1983) 385.
[14] S. Yamamoto, K. Nakanishi and R. Matsuno, *Ion-Exchange Chromatography of Proteins*, Marcel Dekker, New York, 1988.
[15] C.A. Brooks and S.M. Cramer, *AIChE J.*, 38 (1992) 1969.
[16] W. Kopaciewicz, M.A. Rounds, J. Fausnaugh and F.E. Regnier, *J. Chromatogr.*, 266 (1983) 3.
[17] P. Cysewski and G. Jilge, *J. Chromatogr.*, 548 (1991) 61.
[18] F.E. Regnier and I. Mazsaroff, *Biotechnol. Prog.*, 3 (1987) 22.
[19] Y. Li and N.G. Pinto, *J. Chromatogr. A*, 658 (1994) 445.
[20] C.C. Chen and H.I. Britt, *AIChE J.*, 28 (1982) 588.
[21] L.A. Bromley, *AIChE J.*, 19 (1973) 313.
[22] X.H. Lu and G. Maurer, *AIChE J.*, 39 (1993) 1527.
[23] C.C. Chen and L.B. Evans, *AIChE J.*, 32 (1986) 444.
[24] C. Christensen, B. Sander, A. Fredenslund and P. Rasmussen, *Fluid Phase Equilibria*, 13 (1983) 297.
[25] K.S. Pitzer, *J. Phys. Chem.*, 77 (1973) 268.
[26] O. Talu and I. Zwiebel, *AIChE J.*, 32 (1986) 1263.
[27] G.M. Wilson, *J. Am. Chem. Soc.*, 86 (1964) 127.
[28] M.W. Phillips, G. Subramanian and S.M. Cramer, *J. Chromatogr.*, 454 (1988) 1.
[29] E. Glueckauf, *Trans. Faraday Soc.*, 51 (1955) 1540.
[30] D. Kahaner, C. Moler and S. Nash, *Numerical Methods and Software*, Prentice-Hall, Englewood Cliffs, NJ, 1989.
[31] D. Bentrop and H. Engelhardt, *J. Chromatogr.*, 556 (1991) 363.
[32] M.A. Rounds and F.E. Regnier, *J. Chromatogr.*, 283 (1984) 37.
[33] O. Talu, *Ph.D. Dissertation*, Arizona State University, Tempe, AZ, 1984.
[34] Y.H. Ma and Y.S. Lin, *AIChE Symp. Ser.*, No. 242, 81 (1985) 39.